EUROPEAN ORGANIZATION FOR NUCLEAR RESEARCH

Proposal to the ISOLDE and Neutron Time-of-Flight Committee

(Following HIE-ISOLDE Letter of Intent I-089)

Spectroscopy of single-particle states in ^{107,109,111}Sn through (d, p) transfer reactions

January 5, 2021

J. Cederkäll[1], J. Park[2], G. Carlsson[1], C. Fahlander[1], P. Golubev[1], A. Idini[1], A. Knyazev[1], A. M. Moro[3], S. Ahn[2], S. Choi[2], K. I. Hahn[2], J. Hwang[2], D. Kim[2], S. Kim[2], Z. Korkulu[2], B. Moon[2], C.-B. Moon[2], T.-S. Park[2], L. Stuhl[2], M. Górska[4], A. Blazhev[5], P. Reiter[5], N. Warr[5], H. O. U. Fynbo[6], M. J. G. Borge[7], J. A. Briz[7], O. Tengblad[7], A. Heinz[8], H. T. Johansson[8], T. Nilsson[8], S. Siem[9], I. Martel[10], P. A. Butler[11], L. P. Gaffney[11], R. Page[11], M. Labiche[12], I. Lazarus[12], S. J. Freeman[13], D. K. Sharp[13], R. Raabe[14]

[1]*Department of Physics, Lund University, Sweden*
[2]*Center for Exotic Nuclear Studies, Institute for Basic Science, Republic of Korea*
[3]*Department for Atomic, Molecular and Nuclear Physics, University of Seville, Spain*
[4]*Nuclear Spectroscopy Department, GSI, Germany*
[5]*Department of Physics, University of Cologne, Germany*
[6]*Department of Physics and Astronomy, Aarhus University, Denmark*,
[7]*Instituto de Estructura de la Materia, CSIC, Madrid, Spain*
[8]*Department of Physics,Chalmers University of Technology, Sweden*
[9]*Department of Physics, University of Oslo, Norway*
[10]*Department of Applied Physics, University of Huelva, Spain*
[11]*Department of Physics, University of Liverpool, United Kingdom*
[12]*UKRI-STFC Daresbury Laboratory, United Kingdom*
[13]*Department of Physics and Astronomy, University of Manchester, United Kingdom*
[14]*Department of Physics and Astronomy, KU Leuven, Belgium*

Spokespersons: Joochun Park (jcpark@ibs.re.kr) and Joakim Cederkäll (joakim.cederkall@nuclear.lu.se)
Contact person: Karl Johnston (karl.johnston@cern.ch)

CERN-INTC-2021-002 / INTC-P-589
05/01/2021

Abstract: We propose to utilize the unique opportunity given by HIE-ISOLDE and the ISOLDE Solenoidal Spectrometer (ISS) to perform a (d, p) transfer experiment on neutron-deficient ^{106,108,110}Sn in inverse kinematics at 8 MeV/u to study single-particle dominated states and neutron shell evolution towards ^{100}Sn.

Requested shifts: 48 shifts (split into 3 runs over 2 or 3 years)
Installation: [ISS + DSSD-only]

1 Introduction

Current models of nuclear structure and reaction phenomena have predominantly been derived from experiments using atomic nuclei close to stability. They must, however, ultimately be able to provide adequate descriptions of the many unstable nuclides that can be reached using accelerated radioactive beams. The region of the nuclear chart around the doubly magic ^{100}Sn provides a specific testing ground in this respect since there are just ten double shell closures within reach for experiments. Only four of these, at ^{100}Sn, ^{132}Sn, ^{48}Ni and ^{78}Ni, are located far from stability and are therefore of special interest in view of the new experimental possibilities. The robustness of the $N = Z = 50$ shells in terms of shell energy gaps, the single-particle description of states, and the interactions of valence nucleons around the ^{100}Sn core provide characteristics of shell structure evolution that should be possible to explain using nuclear models, which eventually also should use a nucleon-nucleon interaction derived from first principles.

In order to investigate shell evolution in the ^{100}Sn region we have in previous experiments at ISOLDE measured electromagnetic transition strengths, using safe-energy Coulomb excitation, in the light even-A Sn isotopes [1–3] and other neighbouring atomic nuclei [4–8]. In contrast to the neutron-rich Sn isotopes, only a moderate decrease in $B(E2)$ values is observed along the chain of even-A Sn isotopes as the shell closure at ^{100}Sn is approached. Measurements using high-energy Coulomb excitation [9–12] confirm this picture. Some of the latest attempts to explain these observations include Monte-Carlo shell model calculations that propose shape evolution in the light Sn isotopes [13]. High-energy knockout reactions have also been used as a tool for spectroscopy of the even light Sn isotopes [14], and rather recently results from inelastic proton scattering experiments, also at high energy, indicate that the plateau in observed $B(E2)$ values for the first 2^+ state in the mass range $A = 106$ to 112 is largely driven by neutron collectivity [15].

However, spectroscopic data on the lightest odd Sn isotopes is scarce. The current available experimental information about these states, for isotopes lighter than ^{111}Sn, is limited to tentative spin-parity assignments for several cases. Hence, it is needed to verify which of these states have single-particle dominated configurations in order to understand the shell evolution in the ^{100}Sn region.

For the lightest isotopes, following the first observation of ^{103}Sn in-beam [16], only one γ-ray transition, at 172 keV [17, 18], has been measured in ^{101}Sn. Theoretically it has been suggested that systematics of single-particle levels can be a manifestation of the monopole effect of the tensor force [19]. Other recent calculations predict nearly-degenerate $5/2^+$ and $7/2^+$ states as candidates for the ground state of ^{101}Sn [20]. Furthermore, the properties of the Sn isotopic chain have been investigated using particle-vibration coupling in nuclear field theory [21] as well as with other first principle methods [22]. The ^{100}Sn region is consequently of significant current theoretical and experimental interest.

2 Physics case

There has been an approximately fifty-year long hiatus in using (d, p) reactions to study single-particle dominated states in the light odd mass Sn isotopes due to technical limi-

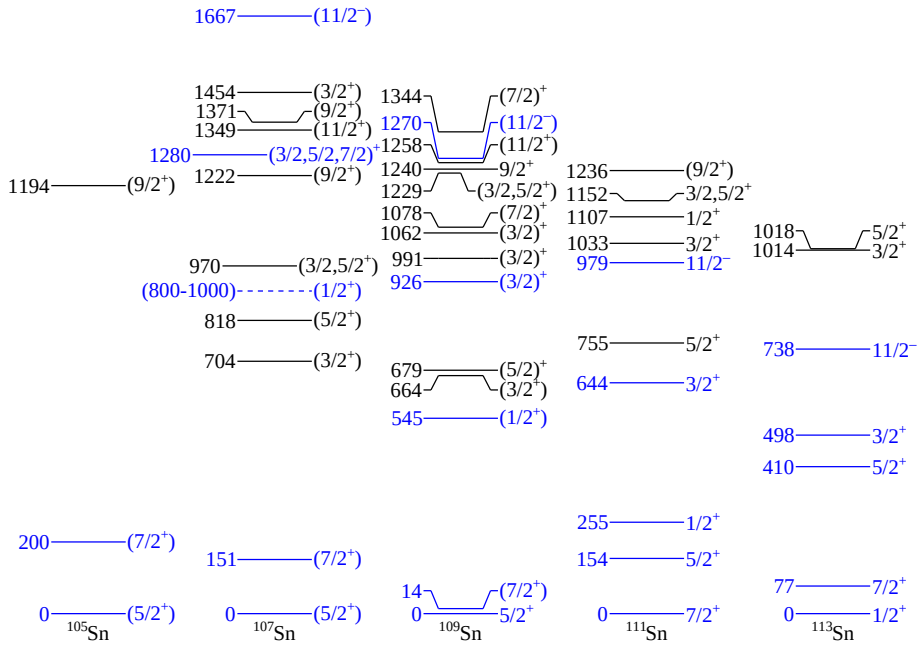

Figure 1: Partial level schemes of light odd-A Sn isotopes. The energy labels on the left side are given in keV. Previously suggested single-particle states in the neutron orbitals between $N = 50$ and $N = 82$ are represented in blue. The spin assignments are taken from Ref. [24].

tations. The latest comprehensive study, e.g. presenting results for ^{113}Sn, was published in 1967 [23]. The proposed experiment will therefore provide the first (d, p) transfer reaction data to characterise the states in the odd unstable light Sn isotopes, and determine to which extent these are neutron single-particle dominated states corresponding to the $2d_{5/2}, 1g_{7/2}, 2d_{3/2}, 3s_{1/2}$ and $1h_{11/2}$ orbits. The level schemes of interest for the current proposal are illustrated in Figure 1. The states presented in the figure were uncovered mainly through β-decay spectroscopy and in fusion-evaporation reactions.

For completeness, one can note that not all yrast states in the level schemes are single-particle dominated configurations. In (d, p) experiments, angular distributions of the outgoing protons are measured and compared to distorted wave Born approximation (DWBA) calculations as a function of orbital angular momentum transfer ΔL. Spectroscopic factors S, between experimental $(d\sigma/d\Omega)$ values and the theoretical prediction, are then determined from the experimental results. The analysis amounts to investigating the energy spectrum and angular distributions in combination, and can include fitting of several states of different angular momenta within a given energy range in order to reproduce the observations. The analysis therefore provides information about potential fragmentation of the strength into several closely lying states. This fragmentation will in turn indicate to what extent presumed single-particle dominated states are indeed such states or if some of the observed states have more collective character. The spins of states of interest discussed below are taken from the latest ENSDF [24], but variations in the certainty of their assignments exist in literature.

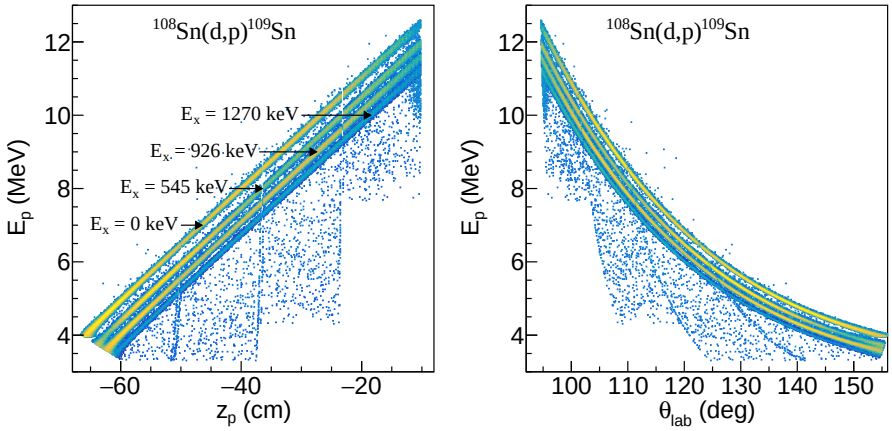

Figure 2: Simulated proton energies as a function of z (left) and θ_{lab} (right) with the proposed ISS setup, from the (d, p) reaction channels to four of the excited states in ^{109}Sn.

The single-particle states of ^{107}Sn have been inferred from a β-decay spectroscopy experiment [26], which could not uncover the $1/2^+$ state which corresponds to a neutron $3s_{1/2}$ configuration. Based on the systematic trend of the yrast $1/2^+$ state energies in odd-mass Sn isotopes, this state may be located between 800 keV and 1000 keV. As shown in Figure 3, the calculated (d, p) cross sections for this state show little dependence on the excitation energy. But the angular distribution analysis may be affected due to overlaps in proton energies from other excited states, in particular the 818-keV and 970-keV states in ^{107}Sn (see Figure 1). The other presumed single-particle states in ^{107}Sn of interest to investigate, are the $(3/2^+)$ and $(11/2^-)$ states at 1280 and 1667 keV, respectively. In addition, the spins and spectroscopic factors of the yrast $(5/2^+)$ and $(7/2^+)$ states in ^{107}Sn have been addressed in a neutron knockout reaction experiment [25], but so far not in a transfer experiment.

The 14-keV gap between the $5/2^+$ and the $(7/2^+)$ states in ^{109}Sn, corresponding to an l-transfer of 2 and 4 respectively, may pose an interesting case for comparisons of spectroscopic factors, where DWBA calculations would depend very little on the kinematics of the reaction. Fine assessments of the optical model potential parameterisations and nuclear deformation in the Sn isotopes may be possible. The tentative assignment of $J^\pi = (1/2^+)$ to the state at 545 keV should be possible to confirm with this experiment, in order to ascertain the systematics of the neutron $3s_{1/2}$ orbital energy and its strength. The same can be said for the $3/2^+$ state at 926 keV with a $\nu d_{3/2}$ configuration [26] and the 1270-keV $(11/2^-)$ state with regards to the $1h_{11/2}$ orbital.

The S values for multiple single-particle and additional states in ^{111}Sn will be compared to those from alternative transfer reactions such as α-transfer reactions on Cd isotopes and neutron pickup reactions on ^{112}Sn [24]. The discrepancies in the S-factors for the $1g_{7/2}$ single-particle ground state of ^{111}Sn [27, 28] will be addressed, and it is also of interest to compare the results from modern theories to the previous calculations performed several decades ago.

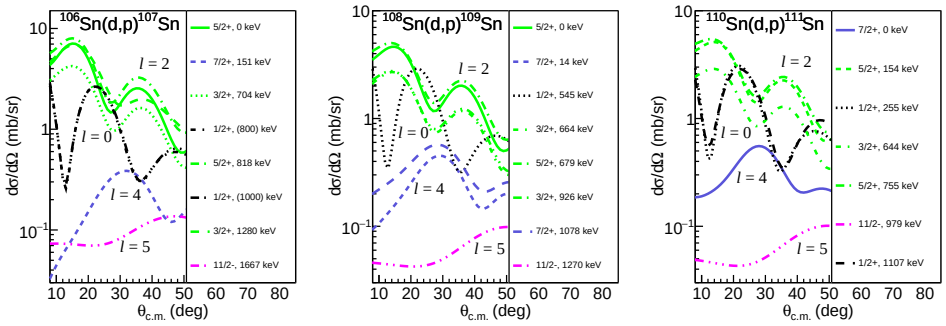

Figure 3: Predicted differential cross sections for (d,p) reactions to the given excited states with orbital angular momenta l in ^{107}Sn (left), ^{109}Sn (center) and ^{111}Sn (right) at $E_{beam} = 8$ MeV/u. See the text for the choice of optical potential parameters in DWBA calculations.

3 Experimental setup

The experiment will performed with the ISOLDE Solenoidal Spectrometer [29] and HIE-ISOLDE. The requested magnetic field strength setting for ISS is 2.5 T. A recoil detector for the outgoing ^{107,109,111}Sn nuclei and tagging of potential isobaric In isotopes for rejection is useful, but based on techniques for isobar suppression developed earlier at HIE-ISOLDE such a detector is not crucial for the latter purpose. The expected Q-value resolution of ISS is about 100 keV, and the Si detector array will cover approximately $8° \leq \theta_{\mathrm{c.m.}} \leq 49°$. In ISS the direction of an outgoing particle is determined by detecting the position along the beam axis, given by the z-coordinate of the setup, where the particle hits a set of Si-strip detectors. For more details about the layout and analysis method applied for ISS we refer to Ref. [29]. A simulation showing laboratory angles and z-position measurements as a function of the proton energies from some of the ^{108}Sn$(d,p)^{109}$Sn reaction channels are shown in Figure 2 as an example. A deuterated polyethylene target with a thickness of 0.165 mg/cm^2 will be used as target, as was done in the IS631 (d,p) experiment on ^{206}Hg [30].

4 Count rate estimates and beam time request

Based on data from our previous experiments, and according to the ISOLDE Yield Database [31], the production yields of ^{106,108,110}Sn from 1.4-GeV protons from the PSB on a LaC_x target, using the RILIS ion source, is 1.6×10^6/uC, 1.4×10^8/uC and 1.8×10^9/uC, respectively [32]. Taking into account EBIS charge breeding and post-acceleration for a typical proton current of 2 μA, intensities of 1×10^5 pps, 5×10^5 pps and 2×10^6 pps can be expected at the CD_2 target for ^{106,108,110}Sn, respectively.
Reaction cross sections for ^{107,109,111}Sn were calculated using FRESCO [33] involving optical model potentials as parameterised in Refs. [34–36] for entrance/exit channels and binding potentials, and are presented in Figure 3. The angular momentum transfer, ΔL, values were assumed to correspond to the neutron orbital angular momenta with

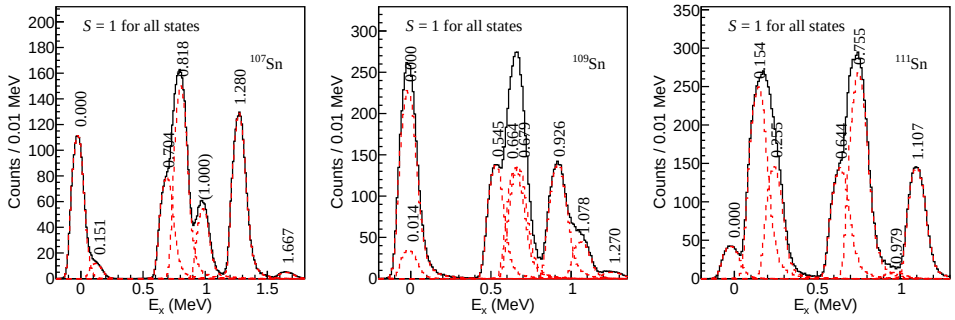

Figure 4: Simulated excitation energy spectra of ^{107}Sn (left), ^{109}Sn (center) and ^{111}Sn (right) from the proposed (d, p) reactions with ISS for a select number of states. A peak for the hypothetical $1/2^+$ state at 1000 keV in ^{107}Sn is also shown. The intensities of individual peaks (red histograms with energy labels) were scaled to match the expected statistics listed in Table 1. The simulation shows the case where the assumed single-particle dominated states also dominate the population probability at their respective energies.

matching J^π values. It was found that beam energies of 8.0 MeV/u yield optimal cross sections for the different states in the three nuclei with different excitation energies and momentum transfers up to 1500 keV. A center-of-mass angular coverage of $8^\circ < \theta_{c.m.} < 49^\circ$ was applied to derive the expected overall cross sections and the resultant proton statistics. The detection efficiency of the Si detectors in ISS is approximately 66%, which is a product of the azimuthal angular coverage of 70% and the Si strip pitch coverage of 94%. The proton counts were further scaled down by a uniform phenomenological quenching factor of 0.55 for nucleon transfer reactions compared to theory, which has been attributed to short-range correlations between nucleons [37]. The predicted event statistics are tabulated in Table 1. The simulations were performed with the ISS NPTool framework [38]. The excitation energy spectra derived from outgoing protons are shown in Figure 4, where the number of events are scaled to the values in Table 1. The energy resolution depends on the CD_2 target thickness, beam spot size (determined to ∼3 mm the x- and y-directions) and the energy spread of the beam (typical ∼0.4-0.5%, but determined to be ∼0.2% for ^{106}Sn at 4.40 MeV/u in 2018). Based on these parameters, the simulated energy resolution was approximately 100-keV FWHM. Isobaric contaminants of In are projected to be a few percent using RILIS for the ^{110}Sn case to up to as much as 50% for ^{106}Sn. However, the effect of isobaric contaminants can, due to the difference in release times between Sn and In, be remedied by beam gate timing with respect to the proton pulse. In addition the laser on/off technique, makes it possible to produce background spectra from any contaminant, that can be subtracted from the data of interest if needed. These techniques were used with good results in the previous Coulomb excitation measurements. Finally, a recoil detector employing ΔE-E measurements, which can operate for event rates up to $\sim 10^5$ pps is planned to be used to provide additional exit channel selection and beam monitoring.
For ^{108,110}Sn, 12 shifts or 96 hours of beam time per isotope are required to generate

Table 1: Calculated (d, p) cross sections and the corresponding proton statistics using ISS for selected states in ^{107,109,111}Sn (see the text for further information).

Reaction/ target	Intensity and beam time	E_x (keV)	J^π	ΔL	σ (mb)	Proton counts
^{106}Sn$(d,p)^{107}$Sn at 8 MeV/u on 165-μg/cm^2 CD_2	1×10^5/s for 24 shifts	0	$5/2^+$	2	4.436	1378
		151	$(7/2^+)$	4	0.461	143
		704	$(3/2^+)$	2	3.444	1070
		818	$(5/2^+)$	2	6.576	2043
		(800-1000)	$(1/2^+)$	0	2.031-2.072	631-644
		1280	$(3/2^+)$	2	5.641	1753
		1667	$(11/2^-)$	5	0.220	68
^{108}Sn$(d,p)^{109}$Sn at 8 MeV/u on 165-μg/cm^2 CD_2	5×10^5/s for 12 shifts	0	$5/2^+$	2	3.893	3018
		14	$(7/2^+)$	4	0.547	424
		545	$(1/2^+)$	0	2.220	1722
		664	$(3/2^+)$	2	2.357	1828
		679	$(5/2^+)$	2	2.411	1869
		926	$(3/2^+)$	2	2.463	1910
		1078	$(7/2^+)$	4	0.750	581
		1270	$(11/2^-)$	5	0.141	109
^{110}Sn$(d,p)^{111}$Sn at 8 MeV/u on 165-μg/cm^2 CD_2	5×10^5/s for 12 shifts	0	$7/2^+$	4	0.685	532
		154	$5/2^+$	2	4.378	3401
		255	$1/2^+$	0	2.346	1822
		644	$3/2^+$	2	2.553	1983
		755	$5/2^+$	2	4.813	3738
		979	$11/2^-$	5	0.147	114
		1107	$1/2^+$	0	2.458	1909

similar proton statistics as for ^{207}Hg discussed in Ref. [30]. In order to account for the lower intensity of ^{106}Sn, 24 shifts are needed for angular distribution analysis. Increasing the thickness of the CD_2 target to 0.250 mg/cm^2 has been considered, but simulations show that the advantage of higher statistics in this case is largely offset by a lower proton energy resolution.

Summary of requested shifts: 12 shifts for ^{110}Sn, 12 shifts for ^{108}Sn and 24 shifts for ^{106}Sn, divided into 3 runs over 2 or 3 years. If prioritisation is needed between the three isotopes, then we suggest that the shifts for ^{110,108}Sn could be adjusted to 8 shifts each which would give similar calculated statistics for the $11/2^-$ state in the three isotopes.

5 Safety aspects

There are no special safety aspects. ISS is a fixed experimental equipment.

References

[1] J. Cederkäll *et al.*, Phys. Rev. Lett. **98**, 172501 (2007).

[2] A. Ekström *et al.*, Phys. Rev. Lett. **101**, 012502 (2008).

[3] J. Park *et al.*, JPS Conf. Proc. **32**, 010036 (2020).

[4] A. Ekström *et al.* Eur. Phys. J. A. **44**, 355 (2010).

[5] A. Ekström, *et al.* Phys. Rev. C **80**, 5 (2009).

[6] D. DiJulio *et al.*, Eur. Phys. J. A **48**, 105 (2012).

[7] D. DiJulio *et al.*, Phys. Rev. C **86**, 3031302 (2012).

[8] D. DiJulio *et al.*, Phys. Rev. C **87**, 017301 (2013).

[9] A. Banu *et al.*, Phys. Rev. C **72**, 061305(R) (2005).

[10] C. Vaman *et al.*, Phys. Rev. Lett. **99**, 162501 (2007).

[11] G. Guastalla *et al.*, Phys. Rev. Lett. **110**, 172501 (2013).

[12] P. Doornenbal *et al.*, Phys. Rev. C **90**, 061302 (2014).

[13] T. Togashi *et al.*, Phys. Rev. Lett. **121**, 062501 (2018).

[14] A. Corsi *et al.* Phys. Rev. C **97**, 044321 (2018).

[15] A. Corsi *et al.* Phys. Lett. B **743** 451 (2015).

[16] C. Fahlander *et al.* Phys. Rev. C **63**,021307(R) (2001).

[17] D. Seweryniak *et al.*, Phys. Rev. Lett. **99**, 022504 (2007).

[18] I. G. Darby *et al.*, Phys. Rev. Lett. **105**, 162502 (2010).

[19] T. Otsuka *et al.*, Phys. Rev. Lett. **95**, 232502 (2005).

[20] T. D. Morris *et al.*, Phys. Rev. Lett. **120**, 152503 (2018).

[21] A. Idini *et al.* Phys. Rev. C **92**, 031304(R) (2015).

[22] P. Arthius *et al.* Phys. Rev. Lett. **125**, 182501 (2020).

[23] E. J. Schneid *et al.* Phys. Rev. **156** 1316 (1967).

[24] Evaluated Nuclear Structure Data File, https://www.nndc.bnl.gov/ensdf/ensdf/ensdf.jsp

[25] G. Cerizza *et al.*, Phys. Rev. C **93**, 021601(R) (2016).

[26] J. J. Ressler *et al.*, Phys. Rev. C **65**, 044330 (2002).

[27] P. J. Blankert, H. P. Block and J. Blok, Nucl. Phys. **A356**, 74 (1981).

[28] E. Gerlic *et al.*, Phys. Lett. **57B**, 338 (1975).

[29] https://isolde.cern/index.php/experiments/isolde-solenoidal-spectrometer-iss

[30] T. L. Tang *et al.*, Phys. Rev. Lett. **124**, 062502 (2020).

[31] ISOLDE Yield Database (Development Version), https://isoyields2.web.cern.ch/YieldByElement_Basic.aspx?Z=50

[32] U. Köster *et al.*, Nucl. Instr. Meth. B **266**, 4229 (2008).

[33] I. Thompson, Comput. Phys. Rep, **7** 167 (1988).

[34] H. An and C. Cai, Phys. Rev. C **73**, 054605 (2006).

[35] A. J. Koning and J. P. Delaroche, Nucl. Phys. **A713**, 231 (2003).

[36] M. Kawai, M. Kamimura and K. Takesako, Prog. Theor. Phys. Suppl. **184**, 118 (1969).

[37] B. P. Kay, J. P. Schiffer and S. J. Freeman, Phys. Rev. Lett. **111**, 042502 (2013).

[38] A. Matta *et al.*, J. Phys. G: Nucl. Part. Phys. **43**, 045113 (2016).

Appendix

DESCRIPTION OF THE PROPOSED EXPERIMENT

The experimental setup comprises: (*name the fixed-ISOLDE installations, as well as flexible elements of the experiment*)

Part of the	Availability	Design and manufacturing
ISS + only CD	☒ Existing	☒ To be used without any modification
[Part 1 of experiment/ equipment]	☐ Existing	☒ To be used without any modification ☐ To be modified
	☐ New	☐ Standard equipment supplied by a manufacturer ☐ CERN/collaboration responsible for the design and/or manufacturing
[Part 2 of experiment/ equipment]	☐ Existing	☒ To be used without any modification ☐ To be modified
	☐ New	☐ Standard equipment supplied by a manufacturer ☐ CERN/collaboration responsible for the design and/or manufacturing
[insert lines if needed]		

HAZARDS GENERATED BY THE EXPERIMENT (if using fixed installation:) Hazards named in the document relevant for the fixed ISS + only CD installation.

Additional hazards:

Hazards	[Part 1 of experiment/ equipment]	[Part 2 of experiment/ equipment]	[Part 3 of experiment/ equipment]
Thermodynamic and fluidic			
Pressure	[pressure][Bar], [volume][l]		
Vacuum			
Temperature	[temperature] [K]		
Heat transfer			
Thermal properties of materials			
Cryogenic fluid	[fluid], [pressure][Bar], [volume][l]		
Electrical and electromagnetic			
Electricity	[voltage] [V], [current][A]		
Static electricity			
Magnetic field	[magnetic field] [T]		
Batteries	☐		
Capacitors	☐		

Ionizing radiation			
Target material [material]			
Beam particle type (e, p, ions, etc)			
Beam intensity			
Beam energy			
Cooling liquids	[liquid]		
Gases	[gas]		
Calibration sources:	□		
• Open source	□		
• Sealed source	□ [ISO standard]		
• Isotope			
• Activity			
Use of activated material:			
• Description	□		
• Dose rate on contact and in 10 cm distance	[dose][mSV]		
• Isotope			
• Activity			
Non-ionizing radiation			
Laser			
UV light			
Microwaves (300MHz-30 GHz)			
Radiofrequency (1-300 MHz)			
Chemical			
Toxic	[chemical agent], [quantity]		
Harmful	[chem. agent], [quant.]		
CMR (carcinogens, mutagens and substances toxic to reproduction)	[chem. agent], [quant.]		
Corrosive	[chem. agent], [quant.]		
Irritant	[chem. agent], [quant.]		
Flammable	[chem. agent], [quant.]		
Oxidizing	[chem. agent], [quant.]		
Explosiveness	[chem. agent], [quant.]		
Asphyxiant	[chem. agent], [quant.]		
Dangerous for the environment	[chem. agent], [quant.]		
Mechanical			

Physical impact or mechanical energy (moving parts)	[location]		
Mechanical properties (Sharp, rough, slippery)	[location]		
Vibration	[location]		
Vehicles and Means of Transport	[location]		
Noise			
Frequency	[frequency],[Hz]		
Intensity			
Physical			
Confined spaces	[location]		
High workplaces	[location]		
Access to high workplaces	[location]		
Obstructions in passageways	[location]		
Manual handling	[location]		
Poor ergonomics	[location]		

Hazard identification:

Average electrical power requirements (excluding fixed ISOLDE-installation mentioned above): [make a rough estimate of the total power consumption of the additional equipment used in the experiment]: ... kW